10th IWA Conference on
INSTRUMENTATION, CONTROL & AUTOMATION
14 - 17 June 2009
Cairns Convention Centre, Cairns, Australia
www.iwa-ica2009.org

# Online monitoring of OUR, $K_L$a and OTE indicators: practical implementation in full-scale industrial WWTPs

I. Irizar[*], J.A. Zambrano[*], D. Montoya[**], M. De Gracia[**] and R. García[***]

[*]CEIT and TECNUN (University of Navarra). Pº de Manuel Lardizabal 15, 20018 San Sebastian (Spain)
(e-mail: iirizar@ceit.es; jazambrano@ceit.es)
[**] ATM S.A. Epele Bailara 29, 20120 Hernani (Spain)
(e-mail: mdegracia@atmsa.com; dmontoya@atmsa.com )
[***] PRAXAIR España S.L. C/ Orense 11, 28020 Madrid (Spain)
(e-mail: rafael_garcía@praxair.com)

**Abstract**
Based on on/off aeration strategies, this paper describes all the steps involved in the development and implementation of three identification algorithms aimed at monitoring the oxygen uptake rate (*OUR*), the oxygen mass-transfer coefficient ($K_La$), and oxygen transfer efficiency (*OTE*) in aerated biological reactors. Firstly, a detailed explanation of the theoretical background behind every algorithm is given. In addition, practical issues have also been taken into account in order to guarantee the quality of estimations. Finally, the three algorithms have been implemented and validated in a full-scale industrial wastewater treatment plant with satisfactory results. Although short-term noise has been observed in the estimated data (especially at high *OUR*s), the medium and long-term data trajectories have been correctly reproduced.
**Keywords**
Aeration; control; diagnosis; monitoring; wastewater

## INTRODUCTION

Unlike large wastewater treatment plants (*WWTP*), small systems (covering both urban and industrial *WWTP*s) are designed using criteria wherein autonomy and minimum maintenance prevail over issues such as advanced monitoring and control. As a consequence, in general: (1) only low-cost instrumentation (e.g., online measurements of dissolved oxygen, redox potential, pH, temperature, flow-rate, water level …) is available in these plants; and, (2) coarse regulation capabilities are preferred (on/off valves, fixed-speed pumps, etc.). Obviously, the above considerations limit the implementation of sophisticated monitoring and control solutions; however, there is no reason why, nowadays, available measurements are being under-exploited in most of these systems, particularly when there are full-scale examples that prove how valuable information for diagnosis can be obtained by processing online data (Lee et al., 2008).

Concerning the industrial sector, although anaerobic digestion has arisen recently as a cost-effective technology for biological carbon removal, aerobic treatments still predominate, particularly when stringent limits on the effluent discharges are imposed. It is widely known that external aeration is an important factor within the total operating costs associated with aerobic treatments. Moreover, the activity of micro-organisms and, therefore, process performance depend strongly on how the external aeration is operated. Thus, the incorporation of aeration control strategies appears essential for two reasons: (1) to save energy costs; and, (2) to guarantee effluent quality.

As mentioned above, in general, industrial *WWTPs* are built with low-cost basic equipment. For aeration control, a common practice within industrial facilities is the utilisation of on/off systems. Clearly, this kind of actuation is not the best means of achieving a fine regulation of the dissolved oxygen (*DO*). Nevertheless, on/off aeration systems can be used beneficially to implement simple *software sensors* for the online monitoring of process indicators such as: (1) the Oxygen Uptake Rate (*OUR*); (2) the oxygen mass-transfer coefficient ($K_La$); and (3) the Oxygen Transfer Efficiency (*OTE*). Thus, the online estimation of these three parameters gives small plants low-cost solutions for the implementation of advanced monitoring and control tools. At present, however, there is no clear confirmation that these indicators are being monitored in full-scale installations. Just a few examples applied to lab/pilot-scale plants can be found in the literature (Puig et al., 2005). This paper describes all the steps involved in the development and implementation of three identification algorithms for online monitoring of the *OUR*, $K_La$ and *OTE* parameters. These algorithms are intended for plants controlled by on/off aeration systems. They have been integrated and validated within *AqquaScan* (Castro et al., 2007), an Internet-based service for the remote monitoring of decentralised *WWTPs*, aimed at providing plant operators with remote access to these parameters.

## DESCRIPTION OF THE IDENTIFICATION ALGORITHMS: THEORETICAL BASIS

### *OUR* and $K_La$ identification algorithms

**Figure 1** shows a theoretical profile of the *DO* trajectories that result from applying on/off strategies for aeration control in a biological tank. For the more general case, the *DO* dynamics in a variable-volume completely-stirred aerated reactor is modelled by equations **[1]**. It can be seen that, four terms have effect on the dynamics of the *DO*: (1) the oxygen transfer rate from external aeration; (2) the oxygen transfer rate across the free surface of the mixed liquor; (3) the oxygen consumption rate by micro-organisms; and (4) the mass transport term.

$$\left.\begin{aligned}\frac{dDO}{dt} &= K_La\cdot(DO_{sat}-DO)+K_La_2\cdot(DO_{sat2}-DO)-OUR+\frac{Q_{in}}{V}(DO_{in}-DO)\\ \frac{dV}{dt} &= Q_{in}-Q_{out}\end{aligned}\right\} \qquad \textbf{[1]}$$

Two coefficients for *DO* saturation have been included ($DO_{sat}$ and $DO_{sat2}$) in order to take into consideration that the composition of the gas used for external aeration (air, pure oxygen …) can differ from that of the gas in contact with the liquid across the free surface (normally, air). In most cases, the second and forth terms in **[1]** are small in comparison to the other two and, therefore, can be neglected. This leads to a simpler formulation as shown by equation **[2],** where the oxygen mass-transfer coefficient $K_La$ depends, among other factors, on the inlet gas flow-rate ($K_La$ = f($Q_{gas}$)).

$$\frac{dDO}{dt} \cong K_La\cdot(DO_{sat}-DO)-OUR \qquad \textbf{[2]}$$

For the particular case of on/off *DO* control strategies (see **Figure 1**), it can be easily deduced that, when aeration is switched off ($Q_{gas} = 0 \rightarrow K_La = 0$), the slope of the *DO* falling trajectory is due to the activity of micro-organisms (i.e., the *OUR* parameter). Therefore, at least theoretically, an online estimation of the *OUR* can be performed by processing the *DO* measurements collected during every sub-interval in which external aeration is off (from now on, *OFF intervals*). Simple linear regression algorithms are particularly appropriate for this purpose because their implementation is straightforward and reliable results are obtained.

By solving **[2]** for those sub-intervals in which aeration is switched on (from now on, *ON intervals*) and on the assumption that $Q_{gas}$ and *OUR*, are both constant during the interval, an exponential trajectory for *DO*, as expressed by equation **[3],** is obtained. In this expression, *OUR* can be assumed to be known since a new value is available at the end of each *OFF* interval. Thus, the only unknown parameter in **[3]** is $K_La$, which can be calculated by fitting **[3]** to the *DO* rising trajectory that takes place in every *ON interval*. $K_La$ identification algorithms have been thoroughly described in previous works. As in the *OUR* estimation, linear regression methods are also valid to estimate $K_La$; however in this case they must be combined with iterative procedures (Suescun et al., 1999).

$$DO(t) = DO_o + \left( DO_{sat} - \frac{OUR}{K_L a} - DO_o \right) \cdot (1 - e^{-K_L a \cdot t}) \qquad [3]$$

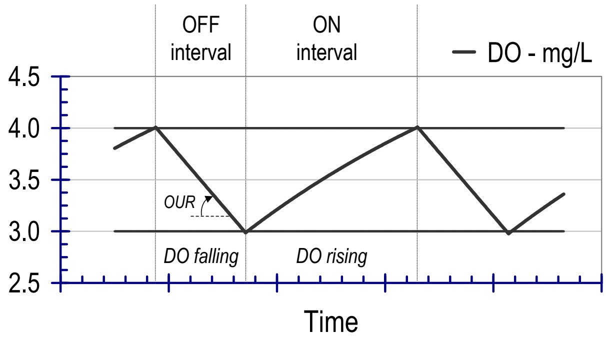


**Figure 1**. On/off aeration control: theoretical *DO* response

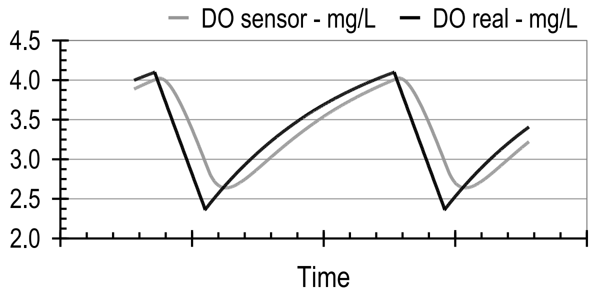


**Figure 2**. On/off aeration control: comparison of sensor and real *DO* trajectories

## *OTE* identification algorithm

In aerated basins, the Oxygen Transfer Efficiency (*OTE*) parameter quantifies the fraction of oxygen from the inlet gas stream that dissolves into the mixed liquor under given process conditions. Off-gas analysis is the most common technique applied in full-scale WWTPs to determine *OTE* in-situ (Leu et al., 2008). However, off-gas methods require specialized equipment and are only applicable to diffused air systems. Moreover, despite the development of cost-effective prototypes in the last few years, this technique remains mostly targeted at medium/large systems. On/off aeration strategies are also of great interest in this case since *OTE* values can be easily calculated using the estimations of $DO_r$ and *OUR*. For a period $\Delta T = t_1 - t_o$ (days) such that *OUR* and *V* are constant and $DO(t_o) = DO(t_1)$, it can be stated that the oxygen transferred to the liquid phase (*OT* - g $O_2$) equals the oxygen consumption by micro-organisms (see equation **[4]**).

$$\int_{t_o}^{t_1} dMO_2 = 0 = \int_{t_o}^{t_1} K_L a \cdot V \cdot (DO_{sat} - DO) \cdot dt - \int_{t_o}^{t_1} OUR \cdot V \cdot dt \rightarrow OT = \int_{t_o}^{t_1} K_L a \cdot V \cdot (DO_{sat} - DO) \cdot dt = OUR \cdot V \cdot \Delta T \qquad [4]$$

Furthermore, if $\Delta T_{on} \in \Delta T$ is the sub-interval where aeration is *ON* and $Q_{gas}$ (assumed constant in $\Delta T_{on}$) is the gas flow-rate ($Nm^3/h$) in this sub-interval, then the mass of oxygen supplied (*OS* – g $O_2$) in $\Delta T$ is obtained by equation **[5]** ($Fr_{O2}$ is the mole fraction of oxygen in the inlet gas):

$$OS = \frac{24 \cdot Q_{gas} \cdot Fr_{O_2} 32 \cdot 101490.8}{8.314 \cdot 293.15} \cdot \Delta T_{on} \qquad [5]$$

Finally, *OTE* (%) can be calculated as the quotient of **[4]** and **[5]**; i.e., the quotient between the oxygen transferred *OT* and the oxygen supplied *OS*, both corresponding to the same period $\Delta T$ (equation **[6]**). The *OTE* identification implements a real-time search algorithm that, in every aeration cycle (i.e., *OFF interval* + *ON interval*), processes the collected *DO* measurements to automatically find values for $\Delta T$, and within it, for $\Delta T_{on}$. Then these values together with the most recent *OUR* value are substituted into **[6]** to determine *OTE*. It can be seen that this algorithm affords small plants a simple and low-cost solution for the online monitoring of *OTE* values.

$$OTE(\%) = \left( \frac{g\,O_2 \text{ dissolved}}{g\,O_2 \text{ supplied}} \right)_{\Delta T} \cdot 100 = \left( \frac{OT}{OS} \right)_{\Delta T} \cdot 100 = \frac{8.314 \cdot 293.15 \cdot OUR \cdot V}{24 \cdot Q_{gas} \cdot Fr_{O_2} \cdot 32 \cdot 101490.8} \cdot \left( \frac{\Delta T}{\Delta T_{on}} \right) \cdot 100 \qquad [6]$$

**Remarks on practical implementation: industrial *DO* sensors**

The implementation of the *OUR* and $K_La$ algorithms shown in the previous section would not be so complicated if commercial *DO* probes had a nearly instantaneous dynamic response. Unfortunately, currently only *DO* instruments for laboratory use seem to present such dynamic properties. In contrast, manufacturers of industrial *DO* sensors prioritise robustness to the detriment of fast time-response. Industrial sensors are not able to follow the real *DO* trajectories that result from the application of on/off strategies for aeration (see **Figure 2**) and, consequently, an estimation of *OUR* and $K_La$ directly based on the *DO* measurements ($DO_m$) leads to erroneous values. This explains in part why the application of these algorithms has been limited to lab-scale studies. A full-scale implementation requires the real *DO* ($DO_r$) to be estimated beforehand. This can be carried out by modelling the dynamic response of *DO* probes. First-order models with dead time, as shown by equation **[7]**, have proved to give satisfactory predictions (Spanjers and Olsson, 1992). In order for the values of $T_c$ (time constant) and $T_m$ (dead time) to be obtained, simple step-response experiments are usually conducted. From the processing of the $DO_m$ signal, its first derivative ($dDO_m/dt$) can be calculated online; then, the values of $DO_m$ and $dDO_m/dt$ can be substituted into **[7]** to predict $DO_r$. Finally, once online $DO_r$ measurements are available, they can be used to estimate *OUR* and $K_La$ as described in the previous section.

$$T_c \frac{dDO_m}{dt} + DO_m = DO_r(t - T_m) \quad [7]$$

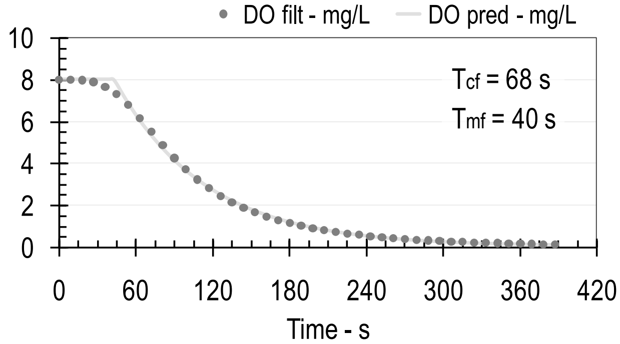


**Figure 3**. *DO* step-response: comparison of real measurements and model predictions after calibration (Hach-Lange LDO sensor)

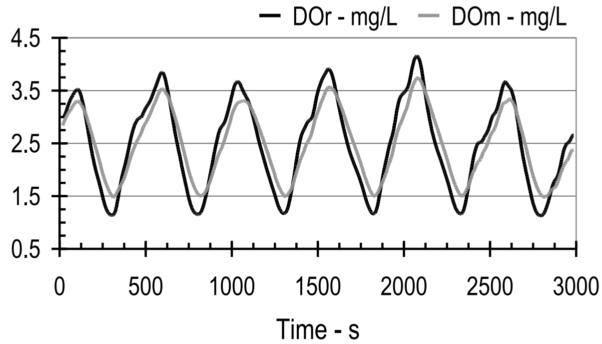


**Figure 4**. Estimation of $DO_r$: comparison of online trajectories for $DO_m$ (sensor) and $DO_r$ (estimation)

**SOFTWARE IMPLEMENTATION**

***DO$_r$* estimation**

In order for the online estimation of $DO_r$ to give satisfactory results, the following adaptations have been required. Since $DO_r$ estimations involve calculating the first derivative of $DO_m$, it has been necessary to implement a low-pass filter for the $DO_m$ sensor signal. Accordingly, a second-order Butterworth digital filter has been designed to ensure full attenuation of high-frequency noise. A natural consequence of filtering is that the dynamic model for the *DO* sensor (**[7]**) has to be reformulated in terms of the filtered signal $DO_{mf}$, which leads to equation **[8]**. Moreover, for every *DO* probe, a step-response experiment has to be conducted. Then, an optimisation algorithm is applied to find the values of $T_{cf}$ and $T_{mf}$ that best fit the model predictions to the experimental results. As an example, **Figure 3** compares, the real and simulated values obtained using a particular Hach-Lange LDO probe, once the model has been calibrated. In addition, **Figure 4** shows the online estimations of $DO_r$ obtained with the calibrated model, using a data set of *DO* measurements collected from the Hach-Lange LDO probe.

$$T_{cf}\frac{dDO_{mf}}{dt}+DO_{mf}=DO_r(t-T_{mf}) \quad \textbf{[8]}$$

### *OUR* and $K_La$ estimation

To improve the robustness of the *OUR* and $K_La$ algorithms, several pre- and post-processing tasks have been introduced. First, a real-time search algorithm to find maximum and minimum values in the $DO_r$ trajectory has been implemented. It guarantees that *OUR* and $K_La$ calculations are performed only with data from the respective $DO_r$ falling and $DO_r$ rising sub-trajectories. Moreover, it has been necessary to set limits for the number of $DO_r$ points required to perform estimations. A minimum limit has been set to ensure that the $DO_r$ trajectory is representative; a maximum limit minimises the effect of changes of either *OUR* or $K_La$ in the interval.

As regards the *OUR* algorithm, a limit value $DO_{min}$ has been set to prevent estimations using low values of $DO_r$. Thus, $DO_r$ values less than $DO_{min}$ are automatically rejected for *OUR* calculations. Considering that *OUR* estimations are calculated on the basis of linear regression methods, the square of the correlation coefficient ($R^2$) has been used as an indicator to quantify the Reliability of Estimations (*RoE* parameter). A limit value $RoE_{min}$ has been set to prevent the storage of erroneous estimations. Thus, only *OUR* estimations whose *RoE* values are greater than $RoE_{min}$ are accepted and, therefore, stored. Finally, the *OUR* algorithm implements an iterative procedure that, for every *OFF interval*, automatically finds those points of the $DO_r$ falling trajectory that give a *RoE* maximum and, in addition, satisfy all the above constraints.

After analysing the shape of multiple $DO_r$ rising trajectories in three different full-scale plants, it was observed that these curves had, in many cases, short and sudden fluctuations. Since the quality of $K_La$ estimations is very sensitive to the presence of these fluctuations, it was decided to modify the algorithm in order to estimate $K_La$ using $DO_{mf}$ trajectories, instead of $DO_r$ trajectories. This meant that **[3]** had to be replaced by a new equation, **[9]**, which expresses the theoretical response of $DO_{mf}$ as a function of $K_La$. Moreover, the Levenberg-Marquardt algorithm (*LMA;* Marquardt, 1963) was implemented to find the $K_La$ values that best fit **[9]** to the $DO_{mf}$ rising trajectories.

Finally, in every *ON interval*, the calculation of $K_La$ is conditional on the availability of a reliable *OUR* value; otherwise, the $K_La$ algorithm is skipped. A more stringent condition is to limit $K_La$ calculations to only those $DO_{mf}$ rising trajectories that fulfil the two following criteria: (1) *OUR* estimations in the preceding and subsequent $DO_r$ falling trajectories are reliable; and (2) both *OUR* values are similar. Such a condition reduces the frequency of $K_La$ estimations but increases the confidence in calculated values (*OUR* can be assumed constant in these cases only). This functionality has not been implemented, however, in the current software release; at present it is under consideration for future versions.

$$DO_{mf}(t)=DO_{st}+(DO_{mf,o}-DO_{st})\cdot e^{-\frac{t}{T_{cf}}}+\frac{DO_{r,o}-DO_{st}}{1-K_La\cdot T_{cf}}\left(e^{-K_La\cdot t}-e^{-\frac{t}{T_{cf}}}\right);\ \text{with}\ DO_{st}=DO_{sat}-\frac{OUR}{K_La} \quad \textbf{[9]}$$

### *OTE* estimation

As in the $K_La$ estimation algorithm, *OTE* calculations are determined by the availability of reliable *OUR* values; otherwise the *OTE* algorithm is skipped. Moreover, since sudden changes of *OUR* negatively affect the quality of *OTE* data, the *OUR* constant condition proposed in the previous section for the $K_La$ algorithm can also be included in this case. Again, this condition will be considered for future implementations. *OTE* estimations are also sensitive to small values of $\Delta T_{on}$;

hence, a minimum limit $\Delta T_{on,min}$ (in units of %ΔT) has been set to prevent the storage of erroneous *OTE* values.

## RESULTS AND DISCUSSION

The three identification algorithms have been implemented and validated in a full-scale Membrane Bioreactor system (*MBR*) treating pharmaceutical wastewater. The *MBR* configuration is made up of two biological tanks with an effective volume of 405 $m^3$ each and working in parallel. For external aeration, both tanks are equipped with a PRAXAIR I-SO™ system (an aeration system based on high-purity oxygen). Two Hach-Lange LDO sensors, one per basin, have been installed to control the *DO* according to an on/off aeration strategy. Other monitored variables are: the reactor temperature, the influent and permeate flow-rates, and the water level. All these measurements can be accessed remotely via the Internet using *AqquaScan* software.

### Online monitoring of $DO_r$

**Figure 5** shows the performance of the on/off *DO* controller as well as the estimation results for the real *DO* ($DO_r$). It should be observed that on/off actions are based on *DO* sensor measurements ($DO_m$), 1 and 2 mg/L, being the lower and upper set-points of the $DO_m$ control band, respectively. The $DO_m$ profile seems to confirm a good regulation of the *DO* level in the reactor, with $DO_m$ values within the aerobic range most of the time, as required for carbon removal. In contrast, $DO_r$ estimations exhibit very low values at the end of the *OFF intervals* (dashed-line circle in **Figure 5**), which evidence that actually the reactor does not work permanently under aerobic conditions and therefore that the process is not being operated efficiently. The large discrepancies between $DO_m$ and $DO_r$ measurements are attributed to two factors: (1) the high organic loading rates applied to the process (≈ 4 kg $COD/m^3 \cdot d$); and (2) the slow dynamic response of the *DO* sensor.

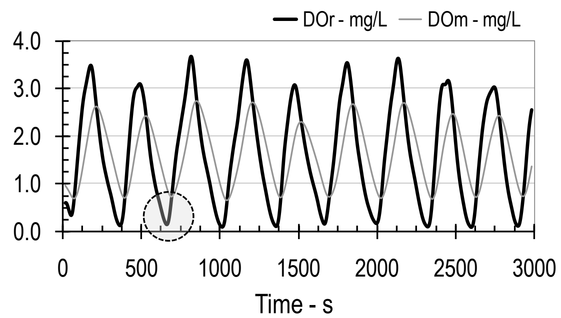


**Figure 5**. Online monitoring of $DO_m$ (sensor) and $DO_r$ (estimation)

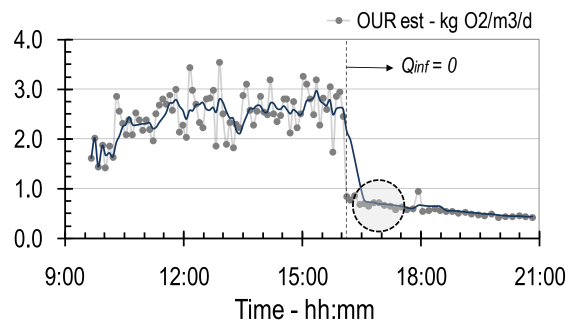


**Figure 6**. Online estimations of *OUR*

In conclusion, the $DO_m$ trajectories that result from on/off aeration strategies do not always reflect the real aerobic conditions present in the process. Thus, the online estimation of $DO_r$ appears crucial in order for plant operators to diagnose and correct abnormal situations which would otherwise remain unobserved. The following two solutions can help to prevent the situation shown in **Figure 5**: (1) narrowing the $DO_m$ control band by increasing the value of the lower *DO* set-point; and (2) implementing the on/off *DO* control strategy using $DO_r$ estimations instead of $DO_r$ measurements.

### Online monitoring of *OUR*

**Figure 6** shows some results on the performance of *OUR* estimations. The larger deviations in *OUR* values take place during the daytime, under normal operation. The cause of these variations can be attributed to two major reasons: (1) short-term fluctuations in the organic load; (2) the greater sensitivity of the identification algorithm to high values of *OUR*. At high *OUR*s, the slope of the

*DO* falling trajectories increases and less $DO_{mf}$ data are available during the *OFF intervals* to estimate *OUR*. In this respect, an automatic *cycle-to-cycle* regulation of the *DO* control band as a function of the *OUR* would help to improve the quality of estimations. In contrast, when influent is interrupted at night, the *OUR* trajectory describes a gradual decrease with practically no oscillations (dashed-line circle in **Figure 6**). In this period, *OUR* values correspond to the *endogeneous* respiration rate and, therefore, they give an estimation of the active biomass present in the mixed liquor.

Additionally, in cases where model-based tools, such as dynamic simulators, assist plant operation endogenous *OUR* is an important parameter for model calibration. Moreover, the gradual decrease of the *OUR* at night periods is linked with reactor temperature and, therefore, allows the dependence of temperature on the endogenous respiration rate to be measured. Due to both the exothermic nature of bio-chemical aerobic transformations and the high organic loads, the reactor temperature increases under normal operation. At night, however, with the feeding pump switched off, the biological heat flux falls sharply and, as a result, the temperature in the tank undergoes a smooth decrease which, obviously, affects *OUR*.

**Online monitoring of $K_La$ and *OTE***

$K_La$ online estimations (**Figure 7**) in general show fluctuations from cycle to cycle that contrast with the application of a constant oxygen gas flow-rate ($Q_{O2} \approx 60$ $Nm^3/h$) during the *ON intervals*. Nevertheless, more than 80% of the estimated values are within the range 100-150 $d^{-1}$. As mentioned above, in every *ON interval* the $K_La$ algorithm uses the values of *OUR*. The current implementation of the $K_La$ algorithm takes this *OUR* value from the preceding *OFF interval*. In this respect, variations in *OUR* from cycle to cycle reduce the quality of $K_La$ measurements. In fact, under normal operation (during the day), deviations in $K_La$ values probably stem from the variations in the *OUR* data. Additionally, the *OUR* algorithm, itself, introduces errors into *OUR* estimations and, hence, into $K_La$ estimations also.

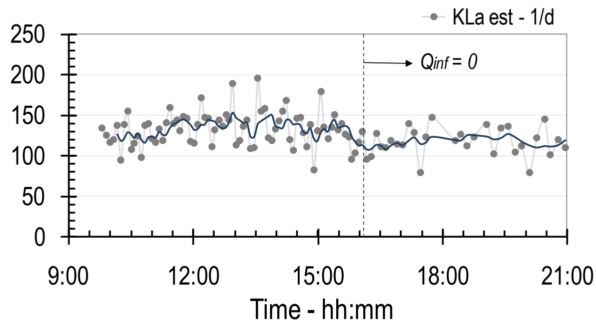


**Figure 7**. Online monitoring of $K_La$

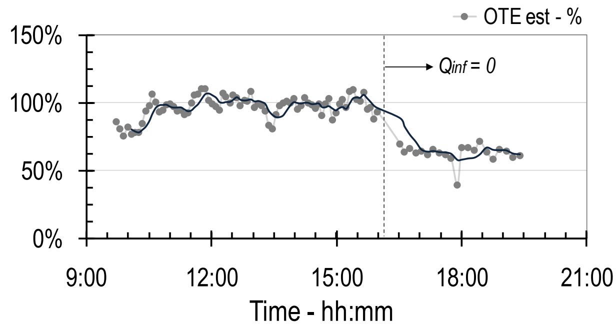


**Figure 8**. Online monitoring of *OTE*

It is worthwhile remarking that, at night, although the variations in *OUR* from cycle to cycle decrease significantly (see **Figure 6**), $K_La$ fluctuations remain. Again, it is not easy to determine with precision the causes of this observation. One of them might be the greater sensitivity of the $K_La$ algorithm to low *OUR* values. At low *OUR*s, the slope of the *DO* rising trajectories increases, and less $DO_{mf}$ data are available to estimate $K_La$. As a solution, an automatic *cycle-to-cycle* regulation of the inlet gas flow-rate (in this case, $Q_{O2}$) as a function of both the *OUR* and the *DO* control band would help to equalise the *DO* rising trajectories.

The *OTE* algorithm is also sensitive to errors in *OUR* measurements (see **Eq. [6]**). This is the reason for the large variations in the *OTE* estimations under normal operation (high *OUR*s). In fact, it can be seen that in this period the current implementation of the *OTE* algorithm sometimes produces erroneous measurements greater than 100% (**Figure 8**). In contrast, during non-feeding periods, the variability of the *OTE* estimations decreases significantly. The comparison of the *OTE* results under normal operation and at night clearly reveals greater efficiencies in the first case. Surprisingly, *OTE* seems to exhibit a certain correlation with the *OUR*. In this respect, further research should be carried out to confirm the above conclusion: firstly, it needs to be proved that the *OTE* identification algorithm, itself, is not connected with such behaviour. Nonetheless, assuming that the *OTE* results are valid, automatic regulation of both the *DO* set-point and $Q_{O2}$ based on the *OUR* can contribute to an improvement in the performance of the plant and to a saving in aeration costs. Under normal operating conditions (high *OUR*s), the *DO* set-point and $Q_{O2}$ should be increased; conversely, at night, during non-feeding periods, the *DO* set-point and $Q_{O2}$ should be decreased.

## CONCLUSIONS

In spite of the fact that small treatment facilities generally employ only low-cost sensors and actuators, the operation of these plants introduces particular functionality such as on/off aeration or non-continuous feeding which, if appropriately exploited, allow enhanced information for plant diagnosis to be collected with no need for extra instrumentation. On/off aeration strategies provide low-cost alternatives for monitoring online the oxygen uptake rate (*OUR*), the oxygen mass transfer coefficient ($K_La$) and the oxygen transfer efficiency (*OTE*). The online monitoring of these three indicators has been carried out in a full-scale industrial *WWTP* with the following conclusions: (1) the actual aerobic conditions in the process can be monitored from the online estimation of the real *DO*; (2) non-continuous feeding periods are suitable for measuring the endogenous respiration rate of micro-organisms; (3) the observed correlation between *OTE* and *OUR* measurements should be investigated in the future. Finally, experimental results have shown that the current implementation of the identification algorithms is especially sensitive to high *OUR* values. It is anticipated that this problem will be overcome in future software releases by incorporating additional signal processing mechanisms that improve the reliability of estimations;

## ACKNOWLEDMENTS

The authors wish to thank the Spanish Ministry of Science and Innovation (CONSOLIDER Program; project NOVEDAR CSD2007-00055) for the financial support of the presented work.

## REFERENCES

Castro A., Sanz J.M., Ayala I., Ayesa E., Alferes J., and Irizar I. (2008). AqquaScan: design and implementation of an Internet-based service for the remote monitoring and management of decentralised WWTPs. *Water Science & Technology*, **57**(10), 1495-1502.

Lee M.W., Hong S.H., Choi H., Kim J-H., Lee D.S., and Park J.M. (2008). Real-time monitoring of small-scaled biological wastewater treatment plants by a multivariate statistical process control and neural network-based software sensors. 2008 . *Process Biochemistry*, **43**, 1107-1113.

Leu S-Y., Rosso D., Jiang P., Larson L.E., and Stenstrom M.K. (2008). Real-time efficiency monitoring for wastewater aeration systems. *Water Practice & Technology*, **3**(3).

Marquardt D.W. (1963). An algorithm for least-squares estimation of nonlinear parameters. *Journal of the Society for Industrial and Applied Mathematics*, **11**(2), 431-441

Puig S., Corominas L., Teresa Vives M., Dolor Balaguer M., and Colprim J. (2005). Development and Implementation of a Real-Time control system for nitrogen removal using OUR and ORP as end points. *Ind. Eng. Chem. Res*. **44**(9), 3367–3373.

Spanjers H., and Olsson G. (1992). Modelling of the dissolved oxygen probe response in the improvement of the performance of a continuous respiration meter. *Water Research*, **26**(7), 945-954.

Suescun J., Irizar I., Ostolaza X., and Ayesa E. (1998). Dissolved oxygen control and simultaneous estimation of oxygen uptake rate in activated-sludge plants. *Water Environment Research*, **70**(3), 316-322.